Processing and Application of Ceramics 10 [2] (2016) 97–105
DOI: 10.2298/PAC1602097K

Promotional effect of nitric acid treatment on CO sensing properties of SnO_2/MWCNT nanocomposites

Nader Kazemi, Babak Hashemi*, Ali Mirzaei

Department of Materials Science and Engineering, Shiraz University, Shiraz, Iran

Received 31 March 2016; Received in revised form 8 June 2016; Accepted 23 June 2016

Abstract

In this paper, SnO_2/MWCNT nanocomposites with different types of MWCNTs, namely as-received, acid treated and Ag-decorated, were synthesized via a facile method and their CO gas sensing properties were investigated. Microstructure and phase formation of the synthesized composites were studied using FE-SEM and XRD, respectively. Fourier transform infrared spectroscopy (FTIR) was employed to study the functional groups on the surface of MWCNTs after acid treatment. CO gas sensing results showed that the samples containing 0.8 wt.% MWCNT with 2 h acid treatment by HNO_3 have the best response to CO gas.

Keywords: *SnO_2, MWCNTs, HNO_3 treatment, Ag precipitation, CO gas sensor*

I. Introduction

Carbon monoxide (CO) is a colourless, tasteless and odourless gas which is notorious as invisible silent killer [1]. It is a highly toxic gas and even in low concentrations death is likely. Indeed, a 10-minute exposure to 5000 ppm concentration is lethal to humans [2,3]. CO is produced mainly by incomplete combustion of organic materials. Risk of exposure to this gas arises from oil or gas burners which are improperly adjusted, for instance from a burning stove or from a burning wood or candles in a closed room [2,3]. This has stimulated considerable interest for researches to develop simple and cheap sensors for the detection of low concentrations of CO gas. Thus, recently many efforts have been devoted to the synthesis of novel sensing materials with high sensitivity towards CO gas [4–6].

SnO_2 is a stable n-type wide band gap semiconductor (E_g = 3.6 eV) and is well-known for potential applications in transparent electrodes, gas sensors, storage applications and solar cells. It is widely used as gas sensor due to its low cost, high sensitivity and simple synthesis procedure [7–11]. In addition, a combination of SnO_2 with carbon nanotubes (CNTs, discovered by Sumio Iijima in 1991 [12]), seems promising for applications in different nanotechnology fields. Thus, large surface to volume ratio, presence of defects, and porous structure of CNTs present effective binding sites for gas molecules. Carbon nanotubes show great potential in making of the next generation sensor technology because they are chemically, thermally, and mechanically very stable. Minimal sensing material requirement and high sensitivity make carbon nanotubes suitable for developing highly sensitive, low power and low cost miniaturized gas sensors. Because of all those advantages, composites of multi wall CNTs (MWCNTs) with other metal oxides have been widely used in sensor technology [13–16]. The selectivity of CNT sensors can be improved either by modifying the nanotube surfaces with desirable functional groups utilizing the selective adsorption of the target molecules on these centres or by developing a nanocomposite architecture consisting of inorganic nanoparticles dispersed in an unfunctionalized MWCNT matrix [17].

The perfect single wall CNT (SWCNT) is without functional groups and therefore chemically quite inert, and CNTs react only to some strong oxidizing or reducing gases due to stable electronic structure. The simplest functionalized SWCNTs were nanotubes with −COOH groups formed upon purification treatment in refluxing HNO_3 [18]. In other words, the sensing capability of CNTs can be increased by sidewall surface modifications such as oxidization, doping, and mechanical deformation [19–23]. Acid treatment or modifying CNTs by HNO_3 or H_2SO_4 leads to formation of functional groups on their surface. This causes the improvement of sens-

* Corresponding author: tel: +98 917 1197591,
fax: +98 3613 415628, e-mail: *hashemib@shirazu.ac.ir*

ing properties, dispersing ability and surface reactivity [22,24,25]. Acid treatment forms some defects on the CNTs surfaces, therefore, the surface adsorbs the gas molecules and it changes the electrical conductivity of CNTs [21,22]. Filling or decorating of CNTs is another way to change their properties [19,21,23].

In this research, SnO_2/MWCNT nanocomposites were synthesized by a low cost conventional method and the effect of different types of MWCNTs (as received, acid treated with HNO_3 and Ag-decorated) on the CO gas sensing properties was investigated. To find the best sensing properties, SnO_2/MWCNTs nanocomposites with different amounts and different types of MWCNTs were fabricated.

II. Experimental procedure

SnO_2 powder (purity >99%, Merck) with average particle size 4–5 μm and MWCNTs (purity >95%) with 10–20 nm in diameter and 5–15 μm in length were used as raw materials. The size of SnO_2 particles was reduced to 50–300 nm by attrition milling with zirconia balls in Teflon vial. Milling was done with ball to powder ratio of 20:1 and rotational speed of 300 rpm in ethanol medium for 2 h.

Acid treated MWCNTs: In order to modify the surfaces of MWCNTs, they were placed in an ultrasonic bath (Luc-405/410/420) containing HNO_3 (99%, Merck) for 1–4 h. Then they were agitated by magnetic stirrer for 2 h at RT. This operation was done to open the top and bottom ends of MWCNTs and to put (−COOH) and (−OH) groups on the MWCNTs surfaces [21,22].

Ag-decorated MWCNTs: To prepare Ag-decorated MWCNTs, 0.05 g of 2 h acid treated MWCNTs were dispersed in 20 ml distilled water by ultrasonic vibration and then 20 ml of silver nitrate (98%, Merck) was gradually added to above suspension and sonicated for 3 h. For precipitation of Ag nanoparticles on the surfaces of MWCNTs, 0.1 molar NaOH (99%, Merck) was added drop by drop to the suspension to reach pH = 10. Subsequently, the Ag-decorated MWCNTs were filtered washed and dried at 75 °C for one hour.

SnO_2/MWCNT nanocomposites: In order to synthesize SnO_2/MWCNT nanocomposites, required amounts of MWCNTs were dispersed in 40 ml ethanol by ultrasonic probe (FS600N) for 15 minutes. Then the milled SnO_2 powder was added to ethanol suspension under ultrasonic vibration for 30 minutes and finally the suspension was placed on magnetic stirrer at 40 °C to evaporate the ethanol. Three different SnO_2/MWCNT nanocomposites were prepared, with the as-received, acid treated and Ag-decorated MWCNTs. Amount of MWCNT (PMWCNT in wt.%) in composites was calculated by the following equation:

$$P_{MWCNT} = \frac{m_{MWCNT}}{m_{MWCNT} + m_{SnO_2}} \quad (1)$$

where m_{MWCNT} is weight of MWCNT and m_{SnO_2} is weight of SnO_2 powder.

After drying of the nanocomposite powder, it passed through a 100-mesh sieve. The pellet samples with diameter of 10 mm and height of 2 mm were made by uniaxial pressing of the powder with pressure of 100 MPa. The samples were put in a quartz tube with the diameter of 15 mm which was evacuated in order to avoid their oxidation during sintering. The samples were sintered at 800 °C for 3 h. Then the surfaces of samples were coated with Ag paste to measure the electrical properties. Resistance was measured at 250 °C in air and in the presence of 50 ppm CO gas. The flow rate and concentration of CO gas were controlled by mass flow controller. The response of sensor (S_R) was defined as the ratio of the resistance of the samples in dry air (R_a) to that in the presence of CO gas (R_g):

$$S_R = \frac{R_a}{R_g} \quad (2)$$

The response time was defined as the time required for the sensor resistance to reach 90% of the equilibrium value after ethanol is injected and recovery time was taken as the time necessary for the sensor resistance to reach 90% of the baseline value in air.

Morphology of the sintered samples was investigated

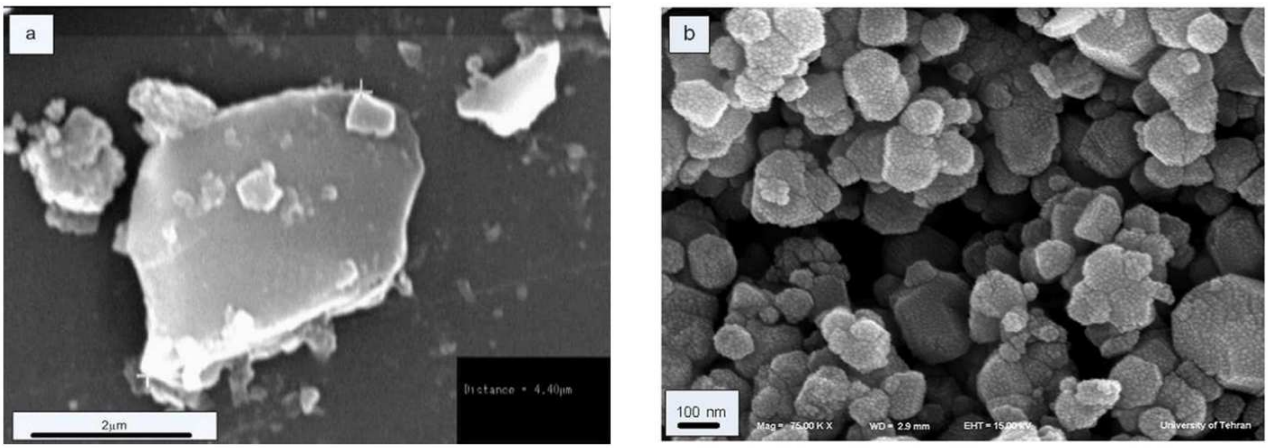

Figure 1. FE-SEM image of SnO_2 powder: a) before and b) after attrition milling

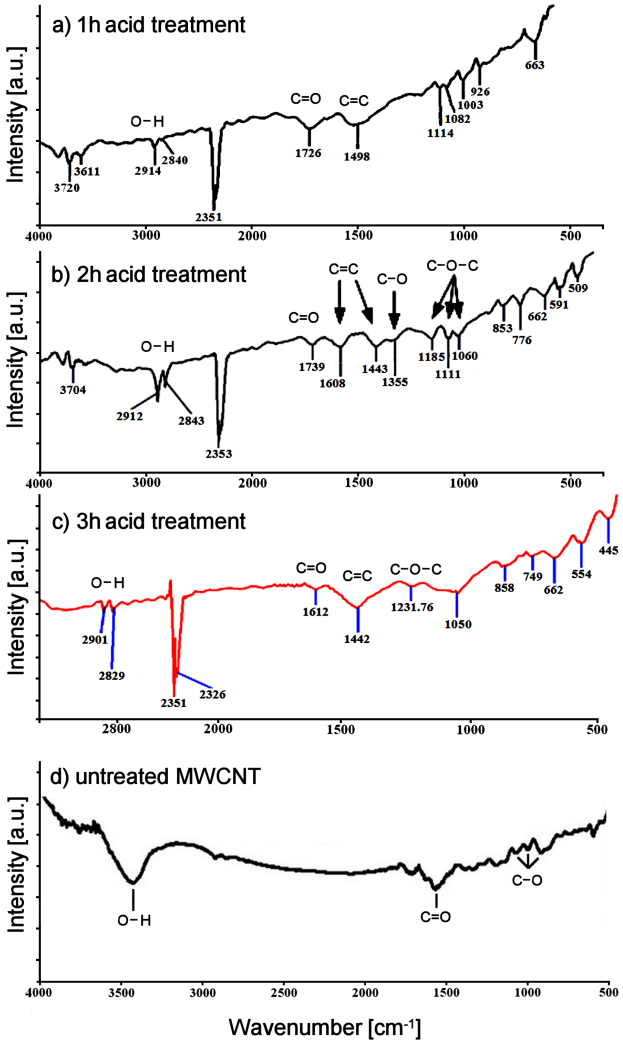

Figure 2. FTIR spectra of MWCNTs after modification by HNO_3 for (a) 1 hour, (b) 2 hours and (c) 3 hours (d) untreated MWCNT (after Tehrani *et al.* [28])

by field emission scanning electron microscopy (FE-SEM, HITACHI-SU70). X-ray diffractometer (Brucker D8 advance) with CuKα radiation (λ = 1.548 Å) was used for the phase analysis of the prepared samples. Fourier transform infrared spectrometer (FTIR, PerkinElmer RX1) was employed in order to study the functional groups formed on the surfaces of MWCNTs.

III. Results and discussion

3.1. Materials characterization

Figure 1a illustrates the FE-SEM micrograph of the untreated SnO_2 powder. As seen, the average particle size of the untreated powders was about 4–5 μm with broad particle size distribution, whereas after attrition milling (Fig. 1b), particle size was in the range of 50–300 nm with some agglomeration. By decreasing the particle size, surface area of powders increases and it is expected that the gas sensitivity will increase accordingly [4].

FTIR spectra of the surface treated MWCNTs (after 1–3 h acid treatment) are shown in Fig. 2. Four peaks in the ranges of 1056–1376 cm^{-1}, 1450–1618 cm^{-1}, 1749 cm^{-1} and 2846–3309 cm^{-1} can be assigned to C–O, C=C, C=O and O–H bonds, respectively [22,26,27]. These peaks show that functional groups have been successfully formed on the surface of MWCNTs after acid treatment. For comparison FTIR spectrum of the unmodified MWCNT without acid treatment is shown in Fig. 2d [28]. As it can be seen, there is no peak due to the presence of the functional groups on the surfaces of the unmodified MWCNT.

Figure 3 shows the morphology of the as-received and Ag-decorated MWCNTs. According to Fig. 3b and EDX analysis, Ag nanoparticles with an average size of about 100 nm have been formed on the surface of MWCNTs.

FE-SEM cross sectional micrograph of the SnO_2/MWCNTs nanocomposite containing Ag-decorated MWCNTs is shown in Fig. 4, where good distribution of MWCNTs in the nanocomposite is noticeable. Good dispersion of MWCNTs is the consequence of the functional group presence at the surface of MWCNTs [23,26].

Figure 5 shows the XRD pattern of the SnO_2/Ag-decorated MWCNTs nanocomposite. As it is seen,

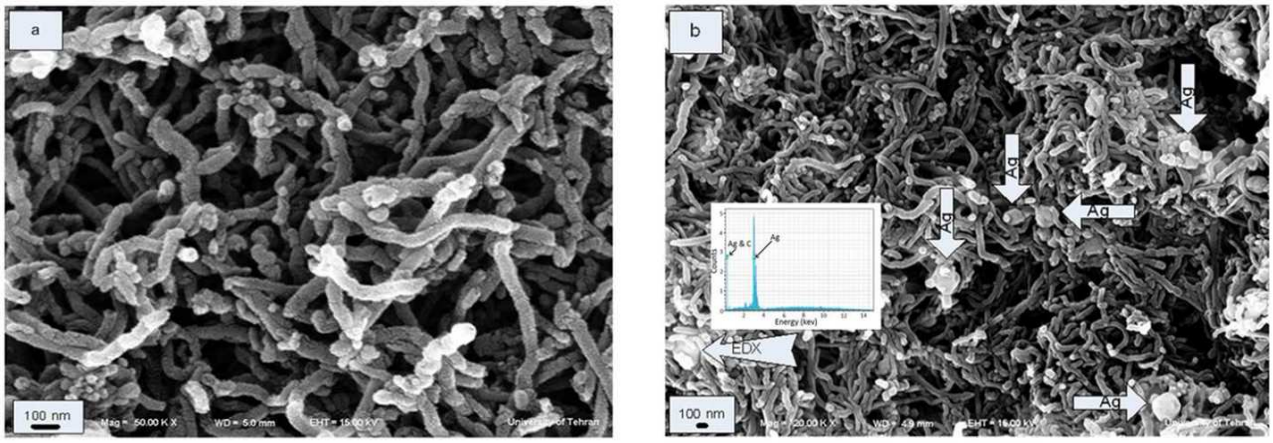

Figure 3. FE-SEM image of MWCNTs: a) before and b) after precipitation of silver nanoparticles

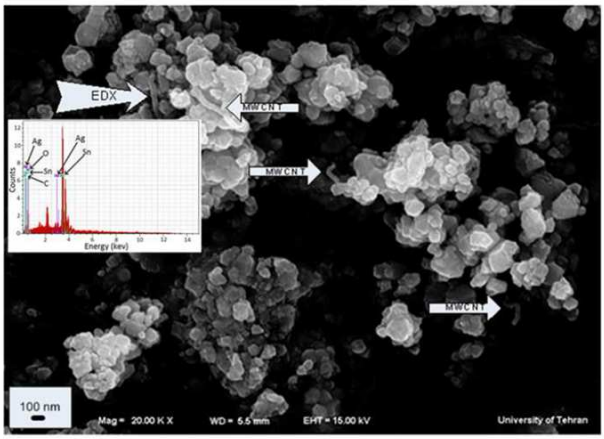

Figure 4. Cross section FE-SEM image of SnO_2/Ag precipitated MWCNTs nanocomposite

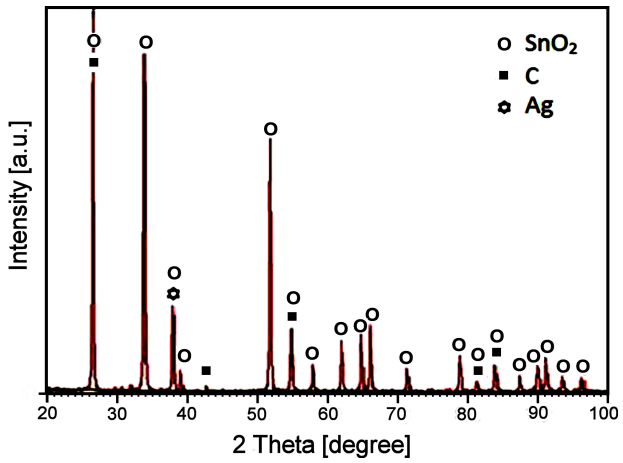

Figure 5. XRD pattern of SnO_2/Ag precipitated MWCNTs nanocomposite

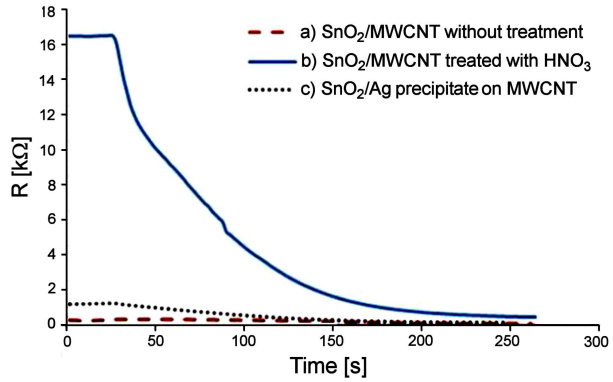

Figure 6. Resistance changes of the samples containing different types of MWCNTs (as-received, acid treated and Ag-decorated) in presence of 50 ppm CO gas

diffraction peaks are related to SnO_2, carbon and silver and other phases are not seen in the pattern. The XRD peaks of MWCNT are positioned at $2\theta = 26.2°$ (002), 44.3° (101) and 54.9° (004).

The peaks centered at 26.5° and 34° were chosen to calculate the crystallite size of the composites by the Scherrer formula [29]:

$$D = \frac{K \cdot \lambda}{\beta \cdot \cos\theta} \tag{3}$$

where D is the crystallite size, K is the shape factor (0.90), λ is the wavelength of X-rays used (1.5406 Å), β is the full-width at half maximum and θ is the diffraction angle in degrees. The average value was about 68 nm.

3.2. Gas sensing properties - Resistance data

Figure 6 shows resistance changes of the samples containing the as-received, acid treated and Ag-decorated MWCNTs in presence of 50 ppm CO gas at 250 °C. Based on the results, the resistance values of the samples containing the as-received and Ag-decorated MWCNTs were in the range of 0.3292–0.048 kΩ ($Ra/Rg = 6.85$), while for the sample containing the acid treated MWCNTs, resistance changed in the range of 16.46–0.464 kΩ ($Ra/Rg = 35.45$). It is obvious that response of the latter sample is much higher than the other two samples. This could be attributed to the presence of functional groups such as C–O, C=O and O–H on the surface of MWCNTs as a result of acid treatment with HNO_3 [21,22].

The gas-sensing behaviour of a semiconductor gas sensor is based on the change in resistance caused by the adsorption and desorption of gas molecules on the surface of the sensor material in the target gas ambience. When the sensor was exposed to air, oxygen molecules were adsorbed on the surface. The adsorbed oxygen molecules extracted electrons from the conduction band of the sensor material, and the electron depletion layer was formed in the surface region, which increased the resistance of the sensors. The reactions can be written as follows:

$$O_{2(gas)} \longrightarrow O_{2(ads)} \tag{4}$$

$$O_{2(ads)} + e^- \longrightarrow O^-_{2(ads)} \tag{5}$$

$$O^-_{2(ads)} + e^- \longrightarrow 2\,O^-_{(ads)} \tag{6}$$

$$O^-_{(ads)} + e^- \longrightarrow O^{2-}_{(ads)} \tag{7}$$

When the nanocomposite sensors were exposed to CO, the CO molecules were chemisorbed on the surfaces of the sensor material, and they reacted with the adsorbed oxygen species to form CO_2 as follows:

$$CO_{(ads)} + O^-_{(ads)} \longrightarrow CO_2 + e^- \tag{8}$$

This led to an increase in electron concentration in the surface region of the sensor material, which eventually decreased the resistivity of the sensor; this decrease in resistivity was used for the detection of CO gas.

Santucci *et al.* [30] reported the interaction between carbon monoxide and hydroxyl modified CNTs. They demonstrated that interaction occurs due to the formation of hydrogen bond between the hydroxyl groups anchored onto CNTs and CO molecules. The bonding behaviour and charge transfer between carbon nanotubes and C–O molecule is illustrated in Fig. 7. The hydro-

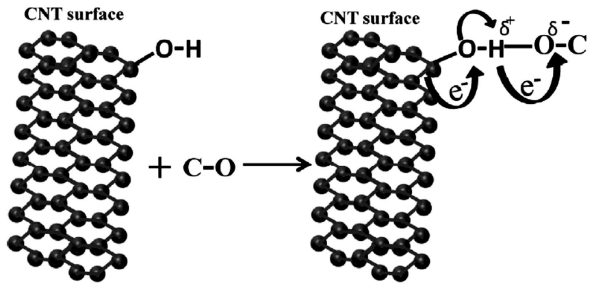

Figure 7. Adsorption of CO gas molecule on the CNTs functionalized with hydroxylgroup. Hydrogen bond is formed between the hydrogen atom of the hydroxyl group and the oxygen atom from carbon monoxide

gen atom of hydroxyl modified CNTs binds with the electronegative oxygen of carbon monoxide. Hydroxyl groups are attached onto CNTs during the purification procedures for the removal of impurities.

Carbon nanotubes due to their strong sp^2 bonding in a near perfect hexagonal network are rather chemically inactive and this prevents the formation of chemical bonds with most molecules. Functionalization of carbon nanotubes improves their chemical reactivity and more adsorption of oxygen takes place at the surface of nanocomposite. Therefore, the thickness of depletion layers or the resistance of sensor increases [13]. In fact CNTs act as a hollow p-type semiconductor with nanochannels. The gas molecules can penetrate within these channels. Therefore, the existence of *p/n* junctions between CNTs and SnO_2 particles and good penetration of gas with inner interfaces increase the sensitivity characteristic of SnO_2/CNTs composite [14]. Dispersion of MWCNTs in SnO_2 powder is one of the most important factors since they have a high tendency for agglomeration.

Decoration of Ag nanoparticles on the surface of nanotubes was not effective in sensing properties of the sample. Decoration of Ag on the surface of acid treated MWCNTs through chemical method may omit the functional groups from the surface of MWCNTs. In addition, the sonication process applied for obtaining a good mixture could separate Ag nanoparticles from MWCNTs. Therefore, the sensing properties of the sample containing Ag-decorated MWCNTs were lower than those for the samples containing the acid treated MWCNTs. This behaviour has been previously reported in literature [20,31].

3.3. Sensing properties - Effect of acid treatment time

Change of resistance with time for the samples containing the acid treated MWCNTs for different periods of time is shown in Fig. 8. The best response is related to the sample containing two hours acid treated MWCNTs. Acid treatment produces functional groups on the surface of MWCNTs, but with increase of acid treatment times, the surface of CNTs can be damaged extensively and decrease the number of functional groups on the surface [32,33]. Khojin *et al.* [34] studied change in the output resistance of CNTs on adsorption of gases. Their studies showed that the output resistance might vary due to changes in potential barrier (i) between the carbon nanotubes and the electrodes, (ii) between interconnected carbon nanotubes, or (iii) due to the variation in the number of charge carriers within the nanotube itself on adsorption of gases. They performed a comparative study between the pristine, slightly defected, and highly defected carbon nanotubes and found that the resistance of the pristine CNTs changed because of variation in the potential either at the junction of two adjacent CNTs or at the metal CNT interconnect. Further, they observed that with increase in the number of defect sites, number of charge carriers in the carbon nanotubes changes. The changes within the carbon nanotubes are responsible for variation in its resistance. They concluded that the gaseous molecules adsorb preferentially on defected CNTs compared to pristine nanotubes [34]. Therefore in our case as acid treatment time was increased up to 2 h probably the number of defects was increased, but after that the surface of MWCNTs was extensively damaged.

3.4. Sensing properties - Effect of MWCNT amount

Changes of resistance with time for the samples containing different amounts of MWCNTs and acid treated

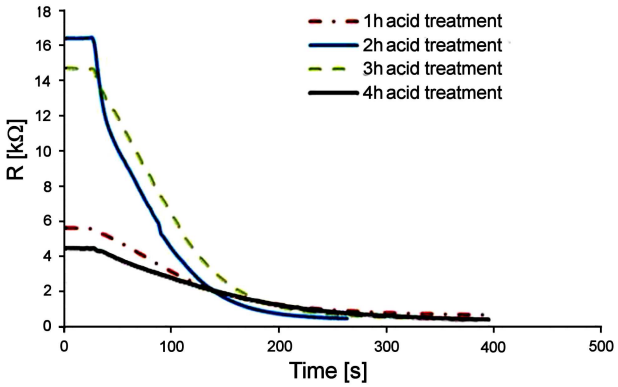

Figure 8. Resistance changes of the samples containing 2 h acid treated 0.8% MWCNTs at different times in presence of 50 ppm CO gas.

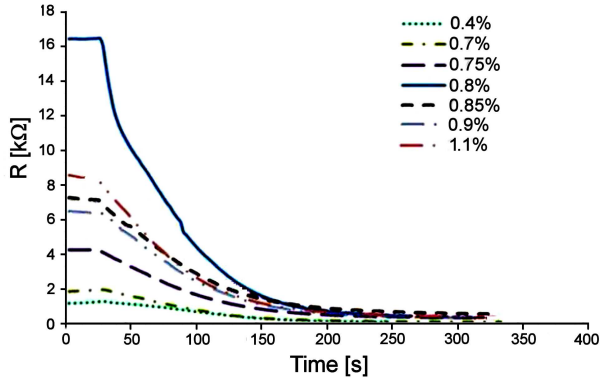

Figure 9. Resistance changes of the samples containing different amount of MWCNTs after 2 h acid treated in presence of 50 ppm CO gas

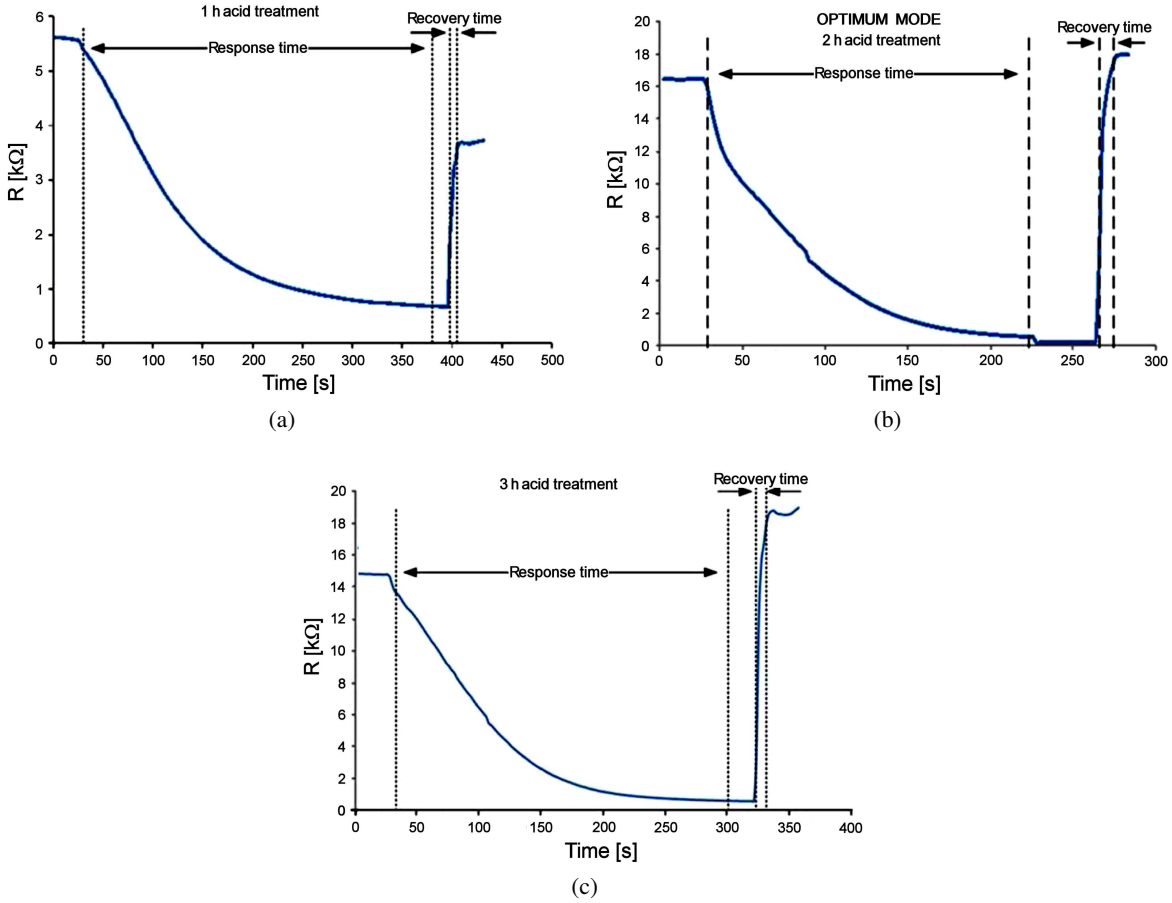

Figure 10. The diagrams of response and recovery times for the SnO_2/0.8% MWCNTs nanocomposite samples containing: a) 1 h, b) 2 h and c) 3 h acid treated MWCNTs

for 2 h are shown in Fig. 9. Adding the acid treated MWCNTs to SnO_2 improves sensing properties of the nanocomposite due to high reactivity with gas and good sensing properties of the acid treated MWCNTs. The best response was obtained in the sample containing 0.8 wt.% MWCNTs. An optimum amount of MWCNTs avoids from percolation of the SnO_2 by the dispersed acid treated nanotubes. However, at high amount of CNTs, resistance decreases because of high conductivity of MWCNTs. A continuous network of CNTs forms when high amount of CNTs is used and this increases conductivity of the nanocomposite [13,31].

Table 1 compares CO gas sensing properties of different metal oxide composites, as it can be seen the present sensor shows good response to 50 ppm CO gas in comparison with other gas sensors. Also in comparison with previous work of the authors about the pristine SnO_2 gas sensor, the present sensor shows better sensitivity.

3.5. Response and recovery times

Response and recovery times of the nanocomposite samples containing 0.8 wt.% MWCNTs acid treated for different times are presented in Fig. 10. The sample containing 2 h acid treated MWCNTs showed the shortest response (200 s) and recovery times (30 s) in comparison to other samples. For all samples there are some drifts but only for this sample, the resistance almost returns to its initial value after stopping of CO gas flow which indicates good stability of this sample [15]. Long response times are probably due to high tortuosity of porous channels in the samples as a result of presence of MWCNTs and short recovery times are due to relatively high working temperature of the sensors.

IV. Conclusions

In a nutshell SnO_2/MWCNT nanocomposites with different types of MWCNT (as-received, acid treatment and Ag-decorated) were synthesized using a simple conventional method. FE-SEM micrograph revealed formation of particles with a size in the ranges of below 100 nm and XRD analysis of the Ag-decorated SnO_2/MWCNT nanocomposite showed presence of Ag, C and SnO_2. Using the as-received MWCNTs and Ag-decorated MWCNTs in comparison with the acid treated MWCNTs did not show good response to CO gas detection in SnO_2/MWCNTs nanocomposite. The best acid treatment time was 2 hours. By increasing acid treatment time of MWCNTs from two to four hours, sensing properties of the SnO_2/MWCNTs nanocomposite decreased due to damaging of nanotubes. The samples containing 0.8 wt.% two hours acid treated MWC-

Table 1. Comparison of CO gas sensing properties of some metal oxide composites

Composite	Synthesis route	Concentration [ppm]	Response (R_a/R_g)	Temperature [°C]	Ref.
CuO/SnO_2-In_2O_3	Chemical route	1000	130	135	[6]
CeO_2 doped SnO_2	Sol-gel	100	4	350	[35]
0.1% CNT on Co_3O_4-SnO_2	Chemical route	600	8 (V_a/V_{gas})	25	[36]
In_2O_3 thin film	Chemical route	1000	25	400	[37]
Proton implanted In_2O_3	Sputtering	1000	8% ($\Delta R/R$)	200	[38]
Co-In_2O_3	RF magnetron sputternig	250	7.5	350	[39]
5 wt.% Eu_2O_3-In_2O_3	Sol-gel	100	1.4	195	[40]
mixed In_2O_3+ZnO	Commercial powders	4600	24	460	[41]
In_2O_3 thin film	Chemical route	500	25	350	[42]
In_2O_3 nanofibers	Electrospinning	100	550% ($\Delta R/R$)	300	[43]
In_2O_3-SnO_2	Sol-gel	50	4	250	[44]
Fe_2O_3-In_2O_3	Sol-gel	50	1.25	350	[45]
MWCNT/SnO_2	Two step mixing	50	16	250	This work
SnO_2	Ball milling	100	5	RT	[46][a]

[a] Previous work of the authors

NTs showed the highest response to 50 ppm CO gas and the shortest response and recovery times.

References

1. T. Yanagimotoa, Y.T. Yu, K. Kaneko, "Microstructure and CO gas sensing property of Au/SnO_2 core-shell structure nanoparticles synthesized by precipitation method and microwave-assisted hydrothermal synthesis method", *Sensor. Actuat. B*, **166-167** (2012) 31–35.
2. P. Patnaik, *A Comprehensive Guide to the Hazardous Properties of Chemical Substances*, John Wiley & Sons Inc., Now York, USA, 2007.
3. P. Warren, *Hazardous Gases and Fumes*, Butterworth-Heinemann, Reed Educational and Professional Publishing Ltd, Oxford, UK, 1997.
4. C.R. Michela, A.H.M. Preciado, R. Parra, C.M. Aldao, M.A. Ponceb, "Novel CO_2 and CO gas sensor based on nanostructured Sm_2O_3 hollow microspheres", *Sensor. Actuat. B: Chem.*, **202** (2014) 1220–1228.
5. Y.T. Yu, P. Dutta, "Examination of Au/SnO_2 core-shell architecture nanoparticle for low temperature gas sensing applications", *Sensor. Actuat. B: Chem.*, **157** (2011) 444–449.
6. H. Yamaura, Y. Iwasaki, S. Hirao, H. Yahiro, "CuO/SnO_2–In_2O_3 sensor for monitoring CO concentration in a reducing atmosphere", *Sensor. Actuat. B: Chem.*, **153** (2011) 465–467.
7. I. Kocemba, S. Szafran, J. Rynkowski, T. Paryjczak, "The properties of strongly pressed tin oxide-based gas sensors", *Sensor. Actuat. B: Chem.*, **79** (2001) 28–32.
8. G. Li, S. Kawi, "MCM-41 modified SnO_2 gas sensors: Sensitivity and selectivity properties", *Sensor. Actuat. B: Chem.*, **59** (1999) 1–8.
9. T.A. Miller, S.D. Bakrania, C. Perez, M.S. Wooldridge, "Nanostructured tin dioxide material for gas sensor applications", *Funct. Nanomater.*, **30** (2006) 453–475.
10. C. Wang, L. Yin, L. Zhang, D. Xiang, R. Gao, "Metal oxide gas sensors: sensitivity and influencing factors", *Sensors*, **10** (2010) 2088–2106.
11. V.E. Bochenkov, G.B. Sergeev, "Sensitivity selectivity and stability of gas-sensitive metal-oxide nanostructures", *Met. Oxid. Nanostruct. Appl.*, **3** (2010) 31–52.
12. S. Iijima, "Helical microtubules of graphitic carbon", *Nature*, **354** (1991) 56–58.
13. R. Leghrib, A. Felten, J.J. Pireaux, E. Llobet, "Gas sensors based on doped-CNT/SnO_2 composites for NO_2 detection at room temperature", *Thin Solid Films*, **520** (2011) 966–970.
14. N.V. Hieu, N.A.P. Duc, T. Trung, M.A. Tuan, N.D. Chien, "Gas-sensing properties of tin oxide doped with metal oxides and carbon nanotubes: A competitive sensor for Et(OH) and liquid petroleum gas", *Sensor. Actuat. B: Chem.*, **144** (2010) 450–456.
15. B. Ghadda, F. Berger, J.B. Sanchez, C. Mavon "Detection of O_3 and NH_3 using tin dioxide/carbon nanotubes based sensors: Influence of carbon nanotubes properties onto sensor's sensitivity", *Procedia Eng.*, **5** (2010) 115–118.
16. H. Liu, H. Ma, W. Zhou, W. Liu, Zh. Jie, X. Li, "Synthesis and gas sensing characteristic based on metal oxide modification multi wall carbon nanotube composites", *Appl. Surf. Sci.*, **258** (2011) 1991–1994.
17. R. Smajda, Z. Györi, A. Sápi, M. Veres, A. Oszkó, J. Kis-Csitária, Á.Kukovecz, Z. Kónya, I. Kiricsi, "Spectroscopic studies on self-supporting multi-wall carbon nanotube based composite films for sensor applications", *J. Mol. Struct.*, **834** (2007) 471–476.
18. H. Kuzmany, A. Kukovecz, F. Simon, M. Holzwe-

ber, Ch. Kramberger, T. Pichler, "Functionalization of carbon nanotubes", *Synthetic Met.*, **141** (2004) 113–122.
19. L. Zhao, L. Gao, "Filling of multi-walled carbon nanotubes with tin(IV) oxide", *Carbon*, **42** (2004) 3251–3272.
20. R. Leghrib, R. Pavelko, A. Felten, A. Vasilieva, C. Canéc, I. Gràciac, J.J. Pireaux, E. Llobet, "Gas sensors based on multiwall carbon nanotubes decorated with tin oxide nanoclusters", *Sensor. Actuat. B: Chem.*, **145** (2010) 411–416.
21. H. Jiang, L. Zhu, K.S. Moon, C.P. Wong, "The preparation of stable metal nanoparticles on carbon nanotubes whose surfaces were modified during production", *Carbon*, **45** (2007) 655–661.
22. E.B. Barros, A.G. Souza Filho, V. Lemos, J. Mendes Filho, S.B. Fagan, M.H. Herbst, J.M. Rosolen, C.A. Luengo, J.G. Huber, "Charge transfer effects in acid treated single-wall carbon nanotubes", *Carbon*, **43** (2005) 2495–2500.
23. P. Corio, A.P. Santos, P.S. Santos, M.L.A. Temperini, V.W. Brar, M.A. Pimenta, M.S. Dresselhaus, "Characterization of single wall carbon nanotubes filled with silver and with chromium compounds", *Chem. Phys. Lett.*, **383** (2004) 475–480.
24. S.W. Kim, T. Kim, Y.S. Kim, H.S. Choi, H.J. Lim, S.J. Yang, Ch.R. Park, "Surface modifications for the effective dispersion of carbon nanotubes in solvents and polymers", *Carbon*, **50** (2012) 3–33.
25. I.D. Rosca, F. Watari, M. Uo, T. Akasaka "Oxidation of multiwalled carbon nanotubes by nitric acid", *Carbon*, **43** (2005) 3124–3131.
26. J. Zhang, H. Zou, Q. Qing, Y. Yang, Q. Li, Zh. Liu, X. Guo, Z. Du, "Effect of chemical oxidation on the structure of single-walled carbon nanotubes", *J. Phys. Chem. B*, **107** (2003) 3712–3718.
27. B. Scheibe, E. Borowiak-Palen, R.J. Kalenczuk, "Oxidation and reduction of multiwalled carbon nanotubes - preparation and characterization", *Mater. Charact.*, **61** (2010) 185–191.
28. M.S. Tehrani, P.A. Azar, P.E. Namin, S.M. Dehghani, "Removal of lead ions from wastewater using functionalized multiwalled carbon nanotubes with tris (2-aminoethyl) amine", *J. Environ. Prot.*, **4** (2013) 1–8.
29. S. Liu, M. Xie, Y. Li, X. Guo, W. Ji, W. Ding, "Synthesis and selective gas-sensing properties of hierarchically porous intestine-like SnO_2 hollow nanostructures", *Mater. Chem. Phys.*, **123** (2010) 109–113.
30. S. Santucci, S. Picozzi, F.D. Gregorio, L. Lozzi, C. Cantalini, L. Valentini, J.M. Keny, B. Delley, "NO_2 and CO gas adsorption on carbon nanotubes: experimentand theory", *J. Chem. Phys.*, **119** (2003) 10904–10910.
31. R. Ionescu, E.H. Espinosa, R. Leghrib, A. Felten, J.J. Pireaux, R. Erni, G. Van Tendeloo, C. Bittencourt, N. Canellas, E. Llobet, "Novel hybrid materials for gas sensing applications made of metal-decorated MWCNTs dispersed on nano-particle metal oxides", *Sensor. Actuat. B: Chem.*, **131** (2008) 174–182.
32. Z. Talaei, A.R. Mahjoub, A.M. Rashidi, A. Amrollahi, M.E. Meibodi, "The effect of functionalized group concentration on the stability and thermal conductivity of carbon nanotube fluid as heat transfer media", *Int. Commun. Heat Mass Transfer*, **38** (2011) 513–517.
33. Y. Ch. Chiang, W.H. Lin, Y.Ch. Chang, "The influence of treatment duration on multi-walled carbon nanotubes functionalized by H_2SO_4/HNO_3 oxidation", *Appl. Surf. Sci.*, **257** (2011) 2401–2410.
34. A.S. Khojin, F.K. Araghi, M.A. Kuroda, K.Y. Lin, J.-P. Leburton, R.I. Masel, "On the sensing mechanism in carbon nanotube chemiresistors", *ACS Nano*, **5** (2011) 153–158.
35. F. Pourfayaz, A. Khodadadi, Y. Mortazavi, S.S. Mohajerzadeh, "CeO_2 doped SnO_2 sensor selective to ethanol in presence of CO, LPG and CH_4", *Sensor. Actuat. B: Chem.*, **108** (2005) 172–176.
36. R.J. Wu, J.G. Wu, M.R. Yu, T.K. Tsai, C.T. Yeh, "Promotive effect of CNT on Co_3O_4-SnO_2 in a semiconductor-type CO sensor working at room temperature", *Sensor. Actuat. B: Chem.*, **131** (2008) 306–312.
37. H. Yamaura, T. Jinkawa, J. Tamaki, K. Moriya, N. Miura, N. Yamazoe, "Indium oxide-based gas sensor for selective detection of CO", *Sensor. Actuat. B: Chem.*, **35-36** (1996) 325–332.
38. A. Salehi, "Preparation and characterization of proton implanted indium tin oxide selective gas sensors", *Sensor. Actuat. B: Chem.*, **94** (2003) 184–188.
39. H.-J. Lee, J.-H. Song, Y.-S. Yoon, T.-S. Kim, K.-J. Kim, W.-K. Choi, "Enhancement of CO sensitivity of indium oxide-based semiconductor gas sensor through ultra-thin cobalt adsorption", *Sensor. Actuat. B: Chem.*, **79** (2001) 200–205.
40. X. Niu, H. Zhong, X. Wang, K. Jiang, "Sensing properties of rare earth oxide doped In_2O_3 by a sol-gel method", *Sensor. Actuat. B: Chem.*, **115** (2006) 434–438.
41. L.I. Trakhtenberg, G.N. Gerasimov, V.F. Gromov, T.V. Belysheva, O.J. Ilegbusic, "Conductivity and sensing properties of In_2O_3+ZnO mixed nanostructured films: Effect of composition and temperature", *Sensor. Actuat. B: Chem.*, **187** (2013) 514–521.
42. W.Y. Chung, G. Sakai, K. Shimanoe, N. Miura, D.D. Lee, N. Yamazoe, "Preparation of indium oxide thin film by spin-coating method and its gas-sensing properties", *Sensor. Actuat. B: Chem.*, **46** (1998) 139–145.
43. S.K. Lim, S.H. Hwang, D. Chang, S. Kim, "Preparation of mesoporous In_2O_3 nanofibers by electrospinning and their application as a CO gas sensor", *Sensor. Actuat. B: Chem.*, **149** (2010) 28–33.
44. G. Neri, A. Bonavita, G. Micali, G. Rizzo, E. Callone, G. Carturan "Resistive CO gas sensors based on In_2O_3 and $InSnO_x$ nanopowders synthesized via

starch-aided sol-gel process for automotive applications", *Sensor. Actuat. B: Chem.*, **132** (2008) 224–233.

45. M. Ivanovskaya, D. Kotsikau, G. Faglia, P. Nelli, S. Irkaev, "Gas-sensitive properties of thin film heterojunction structures based on Fe_2O_3-In_2O_3 nanocomposites", *Sensor. Actuat. B: Chem.*, **93** (2003) 422–430.
46. B. Hashemi, R. Atazadegan, "The effect of nano In_2O_3 and ZnO on the CO gas detection of SnO_2 sensor", *J. Ultrafine Grained Nanostruct. Mater.*, **46** (2013) 67–74.